JOURNAL OF MATERIALS SCIENCE 24 (1989) 2461–2466

Thermal fatigue life of glass subjected to air blast quenching

N. KAMIYA, O. KAMIGAITO
Toyota Central Research & Development Laboratories Inc., Nagakute, Aichi-gun, Aichi-ken, Japan

Thermal fatigue life and thermal shock severity with soda-lime–silica glass rods subjected to air blast quenching were measured. On the basis of the data, the validity of prediction-formulae for thermal fatigue life under mechanical load which were previously derived was discussed. The data of thermal fatigue life proved the validity of the derived formulae for slow cooling conditions such by air blast quenching. Moreover, thermal stress induced on the glass rod subjected to air blast quenching was estimated as 22 MPa by using the formulae, and was in good agreement with the value which was calculated on the basis of heat diffusion theory (30 MPa).

1. Introduction

In many high temperature structural applications, ceramic components are subject to thermal stress. Furthermore, mechanical stress which is caused by holding and/or joining are usually applied to the ceramic components besides the thermal stress. Therefore, in using ceramic components at high temperature, the prediction of thermal fatigue life under the presence of mechanical stress must be carried out to improve the reliability.

The methods predicting the thermal fatigue life of ceramics have been presented by some authors [1, 2]. Present authors presented some prediction-formulae of the thermal fatigue life under the absence [3] and the presence [4, 5] of mechanical stress, and proved the validity of the derived formulae by the thermal fatigue experiments using various ceramic materials, which were carried out by water quenching [3–5]. However, the ceramic components in the heat engine scarcely undergo such rapid cooling as water quenching. Therefore, the thermal fatigue life of the ceramics under slow cooling has to be evaluated. The method of impinging gas jet on ceramics was conducted to evaluate the thermal shock severity [6–8] and thermal fatigue life [9]. However, no reports seem to be published on the statistical thermal fatigue life of ceramics under slow cooling.

In the present paper, the thermal fatigue life of ceramics under slow cooling is discussed. The thermal fatigue life of soda–lime–silica glass are measured and the prediction-formulae of thermal fatigue life, which were derived in the previous paper [4], are examined to be valid for the thermal fatigue life under slow cooling.

2. Experimental procedure

2.1. Specimen

Soda-lime–silica glass rods of 4 mm in diameter were used as specimen. The length of the specimen was 75 mm for thermal fatigue test and 40 mm for bending test. A straight notch of 0.5 mm in depth, 0.5 mm in width and 0.25 mm in the tip radius was introduced to the specimen by using #200 diamond wheel. The location of the notch was the centre of the specimen and the notch was made to be perpendicular to the axis.

2.2. Bending test

Fracture strength of the specimens with and without notch were measured by 3-point bending in which a span was 40 mm and a crosshead speed was 0.005 to 5 mm min^{-1}. From these data, Weibull modulus and exponent, n($V = AK_I^n$; V : crack growth rate, K_I: stress intensity factor) was determined.

2.3. Thermal fatigue test

The apparatus of thermal fatigue test is similar to that described in the previous paper [5]. Nine specimens were set up in the specimen holder. The centre of the specimens were cooled by blowing air of 25 ± 3° C through the copper tube of 4 mm inner diameter, immediately after the specimens were transferred from hot zone. The amount of flowing air was 155 l min^{-1} (130 m sec^{-1}). The specimens were set up so that the notch were exposed to the air flow and mechanical load was applied to the opposite side of the notch through a stainless wire connected to a dead weight. The thermal stress induced by air blast quenching and the mechanical tensile stress by dead weight were superimposed at the notch. The holding time of the specimens in the hot zone and cold zone were 30 and 10 min, respectively. The number of cycles at which each specimen broke was recorded on a digital counter connected to each stainless wire. The maximum number of thermal cycles was limited to 1000 in this experiment.

The thermal shock severity, ΔT, which was the temperature difference between the furnace and the atmosphere, was varied from 140 to 220° C. Mechanical

0022–2461/89 $03.00 + .12

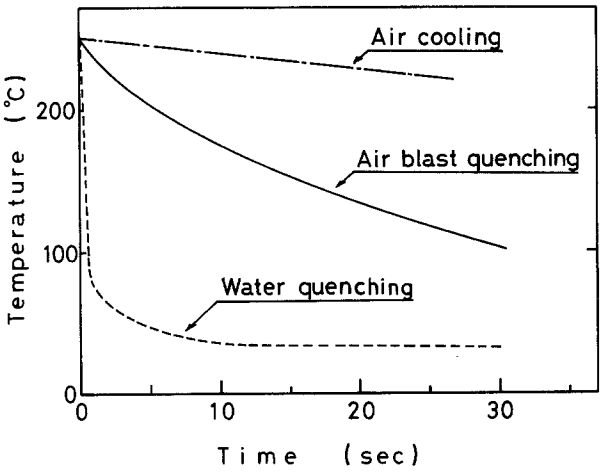

Figure 1 Temperature changes on the surface of copper rod for various cooling condition (air blast quenching, water quenching and air cooling).

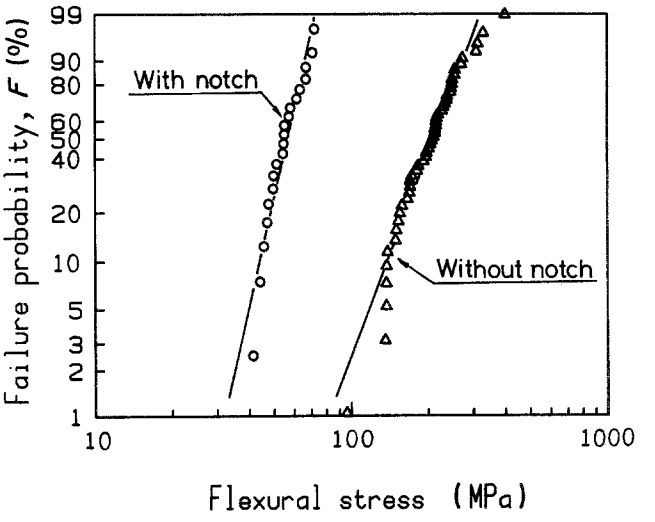

Figure 2 Distributions of flexural strength for soda-lime–silica glass rod with and without notch.

stress, σ_{MO}, which was the maximum bending stress caused by dead weight, was varied from 11.9 to 21.5 MPa. The number of specimens was 9 or 18.

The distribution of fracture temperature difference at which the specimen failed, was studied. In studying the distribution of fracture temperature difference, first thermal shock test was carried out at the lower temperature difference than the minimum of the fracture temperature difference. After the thermal shock, cracks in the specimens were examined using microscope. If no cracking occurred, the temperature difference was increased in 10° C intervals until cracking was observed. The mechanical stress, σ_{MO} of 21.5 MPa was applied to the specimen. The number of specimens was 18.

To evaluate the cooling effect by air blast quenching, the temperature change of the copper rod (5 mm diameter and 75 mm length) with a thermocouple welded on the surface was measured after the copper rod was heated up to 250° C and was exposed to air jet (Fig. 1). The temperature changes were measured in both plunging the copper rod in water at 30° C and keeping that in atmosphere. The temperature changes are 8, 200 and 1° C sec^{-1} for air blast quenching, water quenching and air cooling, respectively.

3. Results

3.1. Flexural strength

The distribution of flexural strength for the specimen with and without the notch is shown in Fig. 2. The average flexural strength and Weibull modulus for the specimens without the notch were 208 MPa and 4.5, respectively. On the other hand, the average flexural strength and Weibull modulus of the specimens with the notch were 55.6 MPa and 7.5, respectively. Introducing the notch decreased the average flexural strength by 73% and increased the Weibull modulus by 66%.

The dependence of the flexural strength of the notched specimen on cross head speed is shown in Fig. 3. From the gradient of the linear line described in Fig. 3, the value of exponent, n is obtained as 15.6, which is in good agreement with the literature values, 16.6 [10] and 17.2 [11].

3.2. Fracture temperature difference

The distribution of fracture temperature difference, ΔT_f for air blast quenching is shown in Fig. 4 for the notched specimens under the presence of the mechanical stress, σ_{MO}, of 21.5 MPa.

The values of fracture temperature difference are widely distributed from 250 to 390° C as well as that of flexural strength. The average value of the fracture temperature differences and the gradient determined by linear regression analysis (Fig. 4) are 299 $\pm$ 32° C and 10.7, respectively.

3.3. Thermal fatigue life

The distributions of thermal fatigue life of the notched specimens subjected to repeated air blast quenching is shown in Fig. 5. Fig. 5a shows those for various temperature difference under a constant mechanical stress, σ_{MO}, of 21.5 MPa and Fig. 5b shows those for various mechanical stress under a constant temperature difference of 220° C. As shown in Figs 5a and b, the datum of thermal fatigue life for constant values of σ_{MO} and ΔT agrees with the fitted lines obtained by linear regression analysis, and the lines for different values of σ_{MO} and ΔT are almost parallel to one another, which are the same with those for soda-lime–silica glass rod subjected to repeated water quenching [4].

4. Discussion

4.1. Thermal fatigue life

In the previous study [4], the formulae for predicting the thermal fatigue life of ceramics under mechanical load have been proposed and the validity of these equations have been proved by measurements of thermal fatigue life of soda-lime–silicon glass rod [4] and sintered mullite rod [5] subjected to repeated water quenching. The prediction-equation are as follows:

$$\ln \ln \left(\frac{1}{1-F}\right) = \frac{m}{n} \ln N + \frac{\ell m}{n} \ln \sigma_{MO} + \frac{(n-\ell)m}{n} \ln \Delta T + C_1 \quad (1)$$

$$\frac{\ell}{n-\ell} \fallingdotseq \frac{\sigma_{MO}}{\sigma_{TO}} = \frac{\sigma_{MO}}{k\Delta T} \quad (2)$$

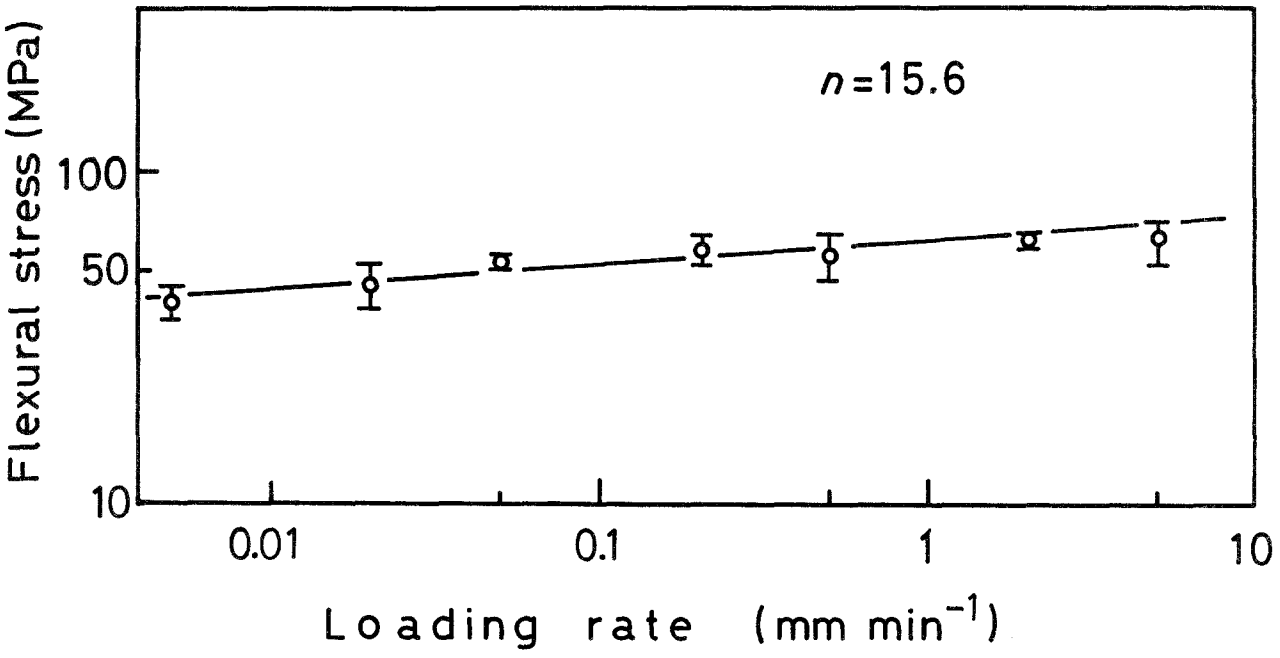

Figure 3 Dependence of flexural strength on stressing rate for soda-lime–silica glass rod with notch.

where F is cumulative failure probability, N is thermal stressing cycle (thermal fatigue life), σ_{MO} is mechanical stress applied to the ceramics, σ_{TO} is maximum thermal stress, n is exponent ($V = AK_I^n$), ℓ is a constant given by a ratio of σ_{MO} and σ_{TO}, and C_1 and k are constants, respectively. From Equation 1, it is understood that $\ln \ln(1/1 - F)$ plotted as a function of $\ln N$ makes a linear line with the gradient of m/n for fixed values of σ_{MO} and ΔT.

As seen in Fig 5a and b, the experimental data for a fixed value of ΔT and σ_{MO} well fits the straight lines determined by the linear regression analysis, and the lines run almost parallel to one another. These linearity and parallelism of the data are considered to prove the validity of the derived prediction-formulae for thermal fatigue life under slow cooling condition as well as rapid one such as water quenching.

For constant values of F and σ_{MO} and those of F and ΔT, the following equations were derived:

$$\ln N \fallingdotseq -(n - \ell) \ln \Delta T + C_2 \quad (3)$$

$$\ln N \fallingdotseq -\ell \ln \sigma_{MO} + C_3 \quad (4)$$

where C_2 and C_3 are constants. Equation 3 and 4 proves linear dependence of $\ln N$ on $\ln \Delta T$ and $\ln \sigma_{MO}$. To examine these relationships, the logarithm of N for $F = 0.5$ on the straight lines in Figs 5a and b are plotted against $\ln \Delta T$ and $\ln \sigma_{MO}$ in Figs 6a and b. As shown in figures, the sets of experimental data fit well straight lines given by linear regression analysis.

The values of n and ℓ determined from Figs 6a and b and Equations 3 and 4, are 25.2 and 11.6, respectively. The value of n, 25.2 is a little larger than that determined from the dependence of flexural strength on stressing rate (15.6). According to Wiederhorn and Bolz [10], the value of n for soda-lime–silica glass which determined from the $K_I - V$ diagram is 16.6 and according to Chandan and co-workers [11], that determined from the dependence of fracture stength on stressing rate is 17.2.

The value of n determined from the thermal fatigue life of the same kind of glass subjected water quench was 25.9 [4] and agrees with that (25.2) determined from the thermal fatigue life by air blast quenching in the present study. Moreover, the value of n determined from the thermal fatigue life of mullite subjected to water quench was a little larger than that determined from the dependence of fracture strength

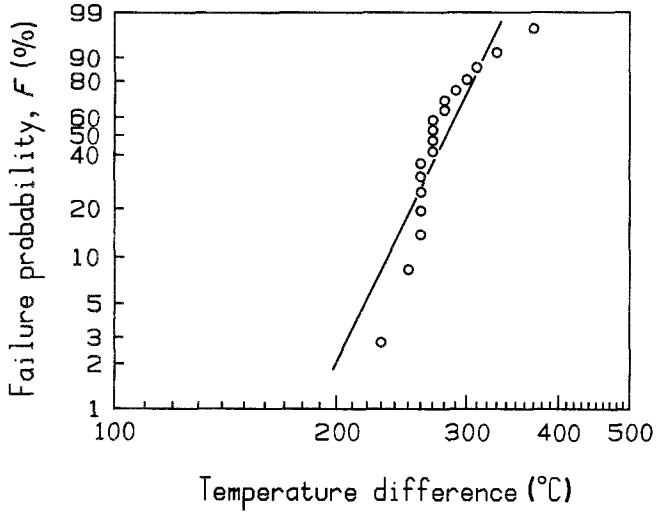

Figure 4 Distribution of fracture temperature difference, ΔT_f for soda-lime–silica glass rod with notch subjected to air blast quenching under the presence of mechanical stress, σ_{MO} (= 21.5 MPa).

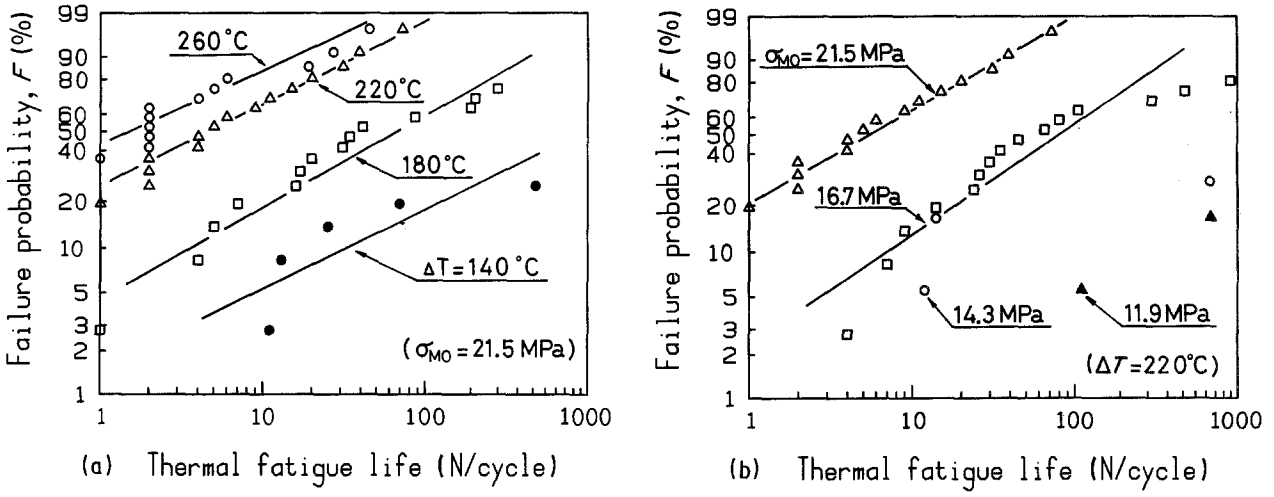

Figure 5 Distributions of thermal fatigue life of notched soda-lime–silica glass rod subjected to repeated air blast quenching for (a) a constant σ_{MO} (21.5 MPa) and (b) a constant ΔT (220° C).

on stressing rate [5], too. Therefore, it is reasonable to consider that the value of n determined from the thermal fatigue life is larger than that determined from the mechanical fracture strength and $K_I - V$ relationships. However, the reason for large value of n is not made clear.

The prediction-formulae of thermal fatigue life, which took account of the dependence of slow crack growth on temperature, can be derived from the prediction formulae which was presented in a previous paper [3], as follows:

$$\ln N - \frac{Q}{RT} \fallingdotseq -(n - \ell) \ln \Delta T + C_2 \quad (5)$$

where Q is the activation energy, R is the gas constant, T is the absolute temperature.

The value of $(n - \ell)$ determined from the present thermal fatigue data using Equation 5 is -2.1. This value can not be accepted because $n \geqq \ell$, which show that the occurrence of large value in n obtained from Equation 3 and thermal fatigue data cannot be attributed to the dependence of slow crack growth rate on temperature.

As described above, the values of n determined from thermal fatigue life are larger than those determined from the dependence of fracture strength on stressing rate and $K_I - V$ relationships, and the large value of n obtained from Equation 3 cannot be attributed to the dependence of slow crack growth rate on temperature. Therefore, it is reasonable to consider that the large value of n obtained from thermal fatigue life is attributed to the fatigue fracture through repeated thermal stress, though the reason for the large value of n is not made clear.

The values of m obtained from the value of n determined from the thermal fatigue data and the gradients, m/n, of the regression line shown in Figs 5a and b are shown in Table I with those obtained from the flexural strength distribution and the values of n determined from various test data. The values of m determined from the thermal fatigue life are 12.1 to 16.3 and 60 to 120% larger than that determined from the flexural strength distribution, 7.5. Notwithstanding the fracture origins were the introduced notches for both the thermal fatigue fracture and bending fracture, both the m values are different as described above. Moreover, the gradient of the regression line for the fracture temperature difference distribution (Fig. 5) is 10.7. According to Equation 1, the critical temperature difference distribution for only one thermal cycling ($N = 1$) is described as follows:

$$\ln \ln \left(\frac{1}{1 - F}\right) \fallingdotseq \frac{(n - \ell)m}{n} \ln \Delta T + \frac{\ell m}{n} \ln \sigma_{MO} + C_1 \quad (6)$$

Equation 6 show that fracture temperature difference distribution gives the straight line whose gradient is $(n - \ell)m/n$. The value of m is obtained as 19.8 from the gradient of the regression line (Fig. 4) and the values of n and ℓ. This value is 2.6 times larger than

TABLE I m, n and l obtained from thermal fatigue life, ΔT_f distribution and flexural strength for notched soda-lime–silica glass rod

Thermal fatigue					ΔT_f distribution	Flexural strength	
Test condition		m	n	l	m	m	n
ΔT (° C)	σ_{MO} (MPa)						
260	21.5	12.6					
220	↑	16.3					
180	↑	14.6					
140	↑	12.1	25.2	11.6	19.8	7.5	15.6
220	16.7	16.8					
↑	14.3	7.6					

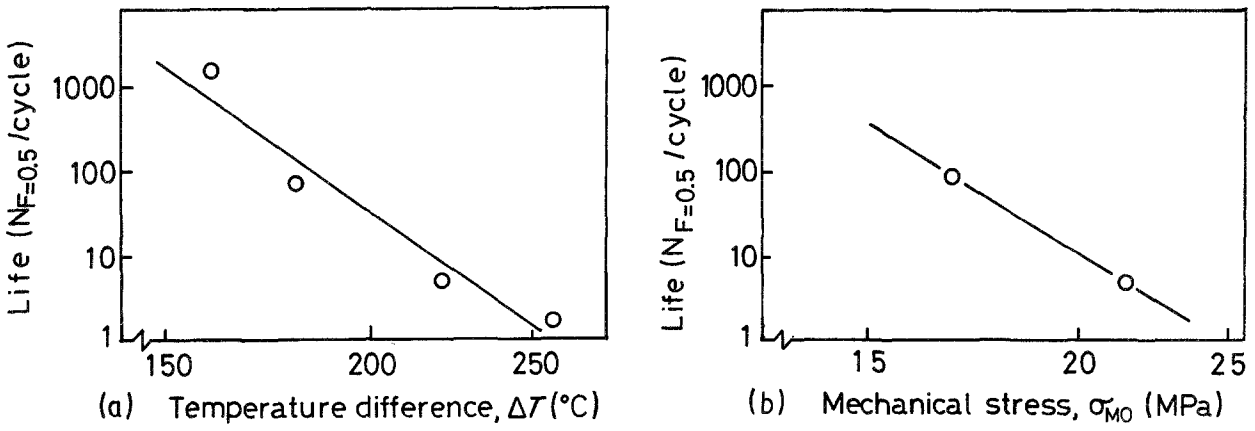

Figure 6 Dependence of thermal fatigue life for notched soda-lime-silica glass rod on (a) temperature difference, ΔT and (b) mechanical stress, σ_{MO}.

that determined from the flexural strength (7.5) and the same as those determined from thermal fatigue life (12.1 to 16.3). As described above, the value of m determined from mechanical flexural strength is different from those determined from thermal fatigue life and critical temperature difference. The reason for this difference was not made clear in the present study, but is considered to be attributed to the difference of the kind of stress, thermal stress and mechanical stress.

4.2. Estimation of thermal stress

By using the values of n (25.2) and ℓ (11.6) obtained from thermal fatigue life and Equation 2, the thermal stress σ_{TO} induced on the surface of the soda-lime-silica glass rod of 4 mm diameter subjected to air blast quenching under the temperature difference of 220° C is estimated as 22 MPa. The sum of the stress induced on the surface of the specimen through the mechanical bending (17 to 22 MPa) and air blast quenching is 39 to 44 MPa. These values agree rather well with the mean value of flexural strength (56 MPa).

Thermal stress on the surface of a cylinder can be analytically estimated as follows [12];

$$\sigma_T(R, t) = \frac{E\alpha\Delta T}{(1-\nu)}\left\{2\sum_{n=1}^{\infty}\frac{J_1(\eta_n)}{(\beta^2+\eta_n^2)J_0^2(\eta_n)} \times [2J_1(\eta_n) - \eta_n J_0(\eta_n)]\exp(-\eta_n^2\kappa t/R^2)\right\} \quad (7)$$

where E is Young's modulus, ν Poisson's ratio, α the coefficient of thermal expansion, β Biot's modulus ($\beta = Rh/k$), R the cylinder radius, h the heat-transfer coefficient, k thermal conductivity, κ thermal diffusivity, J_0 and J_1 the Bessel functions of the zero and first order and η_n the root of $\beta J_0(\eta_n) - \eta_n J_1(\eta_n) = 0$ ($n = 1, 2, 3, \ldots$).

Heat-transfer coefficient, h, is given for a fluid stream flowing against a cylinder as follows [13];

$$h = 0.535\frac{P_r^{0.4}U_j^{0.5}\lambda}{\nu^{0.5}B^{0.5}} \quad (8)$$

where P_r is Nusselt number, U_j the velocity of the air flow, λ thermal conductivity, ν kinematic viscosity and B the diameter of the nozzle from which the air is blown off. The following values were used in the present analysis; $P_r = 0.71$, $U_j = 130\,\mathrm{m\,sec^{-1}}$, $\lambda = 0.022\,\mathrm{kcal\,m^{-1}h^{-1}°C}$, $\nu = 1.56 \times 10^{-5}\,\mathrm{m^2\,sec^{-1}}$. The heat transfer coefficient was calculated as $421\,\mathrm{kcal\,m^2h^{-1}°C^{-1}}$ by using the above described values and Equation 8, and agreed well with the literature value ($432\,\mathrm{kcal\,m^{-2}h^{-1}°C^{-1}}$: air flow rate = $98\,\mathrm{m\,sec^{-1}}$) [14].

The maximum thermal stress is obtained as 30.0 MPa at the time of 1.3 sec. after the start of air cooling by using Equation 7 and the heat transfer coefficient estimated ($421\,\mathrm{kcal\,m^{-2}h^{-1}°C^{-1}}$), and agrees with that (22 MPa) determined from the thermal fatigue data and Equation 2 which was derived by present authors. These facts show that the prediction-formulae of thermal fatigue life for the ceramics under the presence of mechanical stress which have been derived by present authors are applicable not only for the thermal fatigue of the ceramics subjected not only to rapid cooling but also to slow cooling.

5. Conclusions

(1) Experimental examination showed the distribution of thermal fatigue life of soda-lime-silica glass rod subjected to air blast quenching can be presented by Weibull statistics.

(2) The prediction-formulae of thermal fatigue life of ceramics which have been derived were proved to be valid for the thermal fatigue life of ceramics subjected to slow cooling condition.

(3) Thermal stress induced on the glass rod subjected to air blast quenching (25° C) is estimated as 22 MPa, which is in good agreement with the calculated value (30 MPa).

References

1. D. P. H. HASSELMAN, R. BADALIANCE, K. R. McKINNEY and C. H. KIM, *J. Mater. Sci.* **11** (1976) 458.
2. J. P. SINGH, K. NIIHARA and D. P. H. HASSELMAN, *ibid.* **16** (1981) 2789.
3. N. KAMIYA and O. KAMIGAITO, *ibid.* **14** (1979) 573.
4. *Idem, ibid.* **17** (1982) 3149.
5. *Idem, J. Ceram. Soc. Jpn* **93** (1985) 275.
6. M. BUSAWON, B. AUGUSTYNIAK, G. FANTOZZI and D. ROUBY, in "Ceramic Materials and Components for Engines", edited by W. Bunk and H. Haunsner, (SDV Saarbrücker Druckerei und Verlag GmbH, Germany, 1987) pp. 799–806.

7. D. B. MARSHALL, M. D. DRORY, R. L. LOH and A. G. EVANS, in "Fracture in Ceramic Materials, Toughening Mechanism, Machining Damage, Shock", edited by A. G. Evans, (Noyes Publishers, U.S.A., 1984) pp. 336–363.
8. D. JOHNSON-WALLS, M. D. DROY, A. G. EVANS, D. B. MARSHALL and K. T. FABER, *J. Amer. Ceram. Soc.* **68** (1985) 363.
9. J. LAMON, *J. Mater. Sci.* **16** (1981) 2119.
10. S. M. WIEDERHORN and L. H. BOLZ, *J. Amer. Ceram. Soc.* **53** (1970) 543.
11. H. C. CHANDAN, R. C. BRADT and G. E. RINDONE, *ibid.* **61** (1978) 207.
12. R. BADALIANCE, D. A. KROHN and D. P. H. HASSELMAN, *ibid.* (1974) 432.
13. M. KUMADA, I. MABUCHI and Y. KAWASHIMA, *Trans. Japan Soc. Mech. Eng.* **38** (1972) 2915.
14. W. D. KINGERY, H. K. BOWEN and D. R. UHLMANN, "Introduction to Ceramics", 2nd edn (John Wiley & Sons, New York, 1967) p. 822.

Received 17 May
and accepted 12 September 1988